

# Experimental and Computer-aided Investigation of the Image Guide and its Transition to the Standard Metal Rectangular Waveguide

Iliyana I. Arestova, Valda P. Levcheva and Plamen I. Dankov, *Member, IEEE*

**Abstract** — The image guide (IG) has been traditionally considered as a perspective for millimeter wavelengths. The transition between the standard metal rectangular waveguide (SMRW) and the IG usually exists in every experimental set-up involving the IG. Here we have examined experimentally using electric probes the distribution of the electric field components at a double SMRW – IG transition, comprising a dielectric core symmetrically tapered in the H-plane. After that, we have simulated this transition as well as some other transitions using the finite element method (FEM).

**Keywords** — image guide (IG), millimeter wavelengths, transition to IG.

## I. INTRODUCTION

THE image guide (IG) is one of the proposed and intensively investigated structures for millimeter wavelengths [1], [2]. It has been considered not only as a guiding structure with excellent features at millimeter wavelengths, but also as a possible base for design of components, in particular nonreciprocal components (isolators, circulators). The experimental investigations of some nonreciprocal coupled ferrite-dielectric IG structures have been performed in [3], [4]. In order to help the further design of such type of nonreciprocal components, here we have performed experimental and numerical investigation of the IG with an accent on its transition to the standard metal rectangular waveguide (SMRW).

First we have investigated experimentally in the frequency range (30-36) GHz the IG structure, containing two identical transitions between IG and SMRW. The top view of the structure is shown in Fig. 1. Both ends of the IG section made from alumina ( $\epsilon_r = 9.6$ ,  $\text{tg}\delta_\epsilon = 1.10^{-4}$ ) with a cross section 1.80 mm x 0.97 mm have been symmetrically tapered in H-plane. The length of the tapers ( $l = 15$  mm) has been optimized experimentally during some “cut-and-try” procedure. The entire length of the

structure was 80 mm including both transitions.

Following that we have simulated the transitions with lengths from  $l = 5$  mm to  $l = 25$  mm. In addition to the symmetrical configuration (Fig. 2a) we have simulated the asymmetrical one (Fig. 2b) as well.

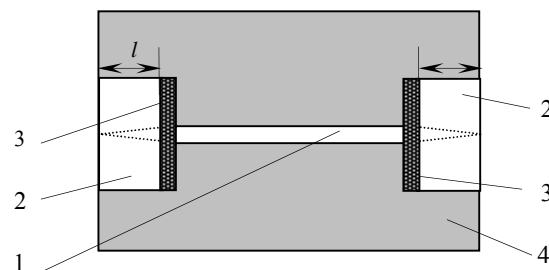


Fig. 1: The top view of the structure under investigation.

1 – IG; 2 – transitions; 3 – absorbing plates; 4 – metal plate;  $l$  – transition length.

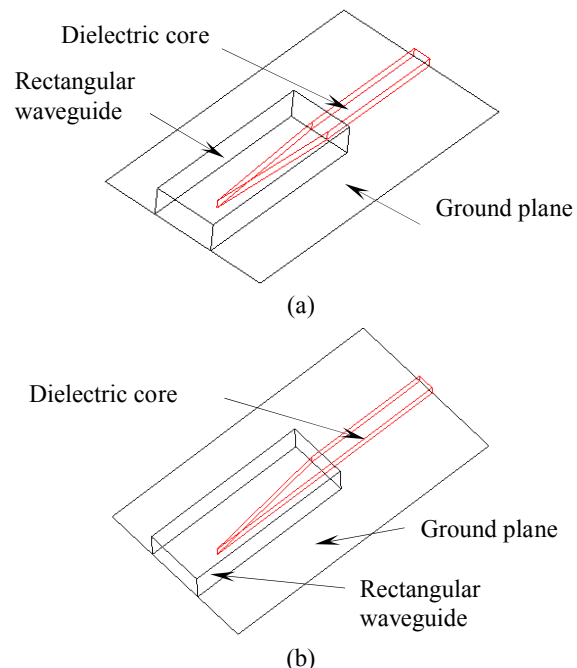


Fig. 2: The symmetrical (a) and asymmetrical (b) transition configurations.

The authors thank the Scientific Research Fund of Sofia University for supporting the investigations.

I. I. Arestova is with the Faculty of Physics, University of Sofia, Bulgaria (phone: 359-2-8161724; e-mail: ilar@phys.uni-sofia.bg).

V. P. Levcheva is with the Faculty of Physics, University of Sofia, Bulgaria (phone: 359-2-8161724; e-mail: levcheva@phys.uni-sofia.bg).

P. I. Dankov is with the Faculty of Physics, University of Sofia, Bulgaria (phone: 359-2-8161806; e-mail: dankov@phys.uni-sofia.bg).

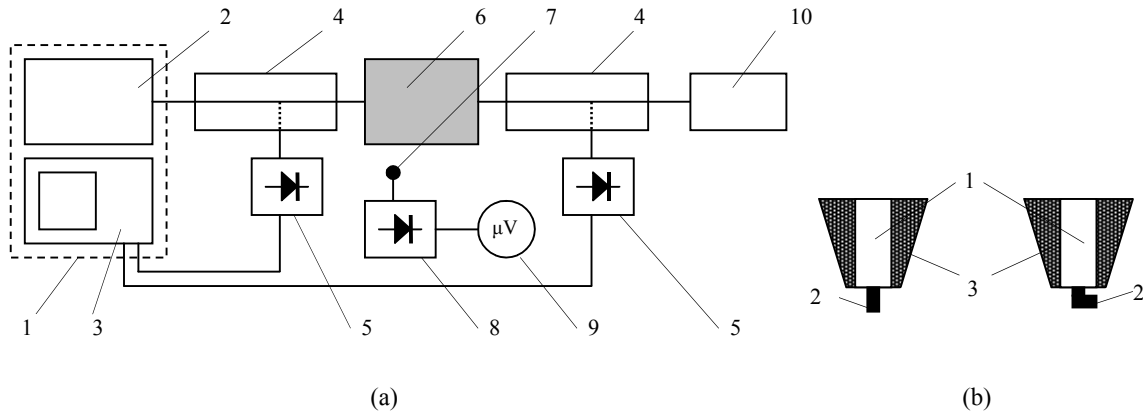


Fig. 3: The experimental setup (a) and the electric probes (b).  
 (a) 1 – scalar network analyzer; 2 – generator; 3 – indicator; 4 – directional couplers; 5 – detectors;  
 6 – the structure under investigation; 7 – electric probe; 8 – detector; 9 – microvoltmeter; 10 – matched load.  
 (b) 1 – semi-rigid coaxial cable; 2 – inner conductor; 3 – absorbing coating.

## II. EXPERIMENTAL INVESTIGATION

The experimental set-up is shown in Fig. 3a. The scalar network analyzer for frequencies from 26 GHz to 38 GHz includes SMRW components with a cross section of 7.2 mm x 3.4 mm. The structure under investigation has shown losses of about 1 – 2 dB in the entire frequency range.

The coaxial electric probes (Fig. 3b) have been successfully used earlier [4], [5] in the electric field sampling. The electric probe shown in the right (Fig. 3b) is used for both of the  $E_x$  and  $E_z$  components at the proper orientation, and the electric probe shown in the left – for the  $E_y$  component. The electric probes for the  $E_x$  and  $E_z$  components contain a 90° bend of the inner coaxial conductor and has been assessed as less perfect than the electric probe for the  $E_y$  component [5]. The electric probe was mounted on a three axes vernier mechanism that permits positioning of the probe with an accuracy of 0.01 mm along the transverse axes  $Ox$  and  $Oy$ , and 0.05 mm along the longitudinal axis  $Oz$ .

The measured distributions of the electric field components at a frequency of 33 GHz are shown in Fig. 4. The quantity along the vertical axis, which is measured in arbitrary units, is proportional to the squared electric field components due to the square-law characteristic of the detector. The origin of the  $x$ -axis is at the middle of the dielectric core of the IG. The distribution of the  $E_y$  component is omitted here because of its similarity to that of the  $E_x$  component, but at a higher level.

As it could be seen from Fig. 4, the distributions are slightly asymmetrical with respect to the plane  $x = 0$ , which is not in accordance with the geometrical symmetry of the structure and at this stage of the investigation has been explained as due to some imperfections of the real structure. At planes  $x = -1$  mm and  $x = 1$  mm there are maxima of both of the  $E_x$  and  $E_z$  components – very slight for the  $E_x$  component and strong enough for the  $E_z$  component. This could imply, that the non-principal components  $E_x$  and  $E_z$  seem to be more essential in the vicinity of the dielectric core's side walls. The standing wave pattern observed corresponds to the standing wave

ratio SWR of about 1.1 and the guide wavelength  $\lambda_g$  of about 5.7 mm.

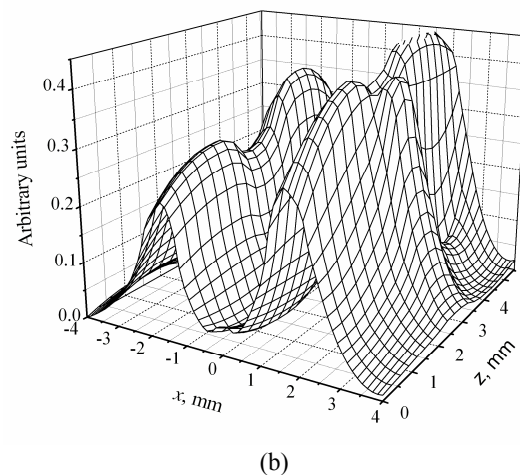
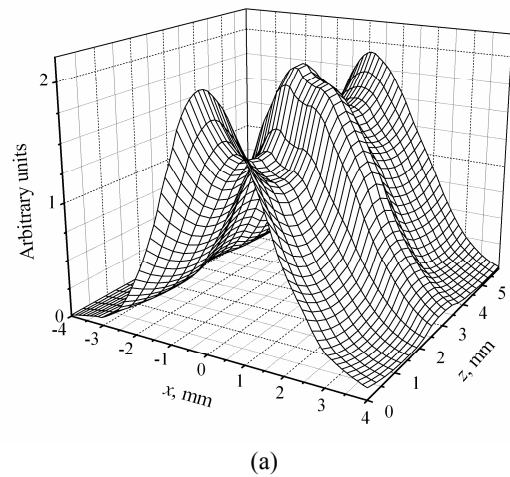


Fig. 4: The measured distributions of the  $E_x$  (a) and  $E_z$  (b) components.

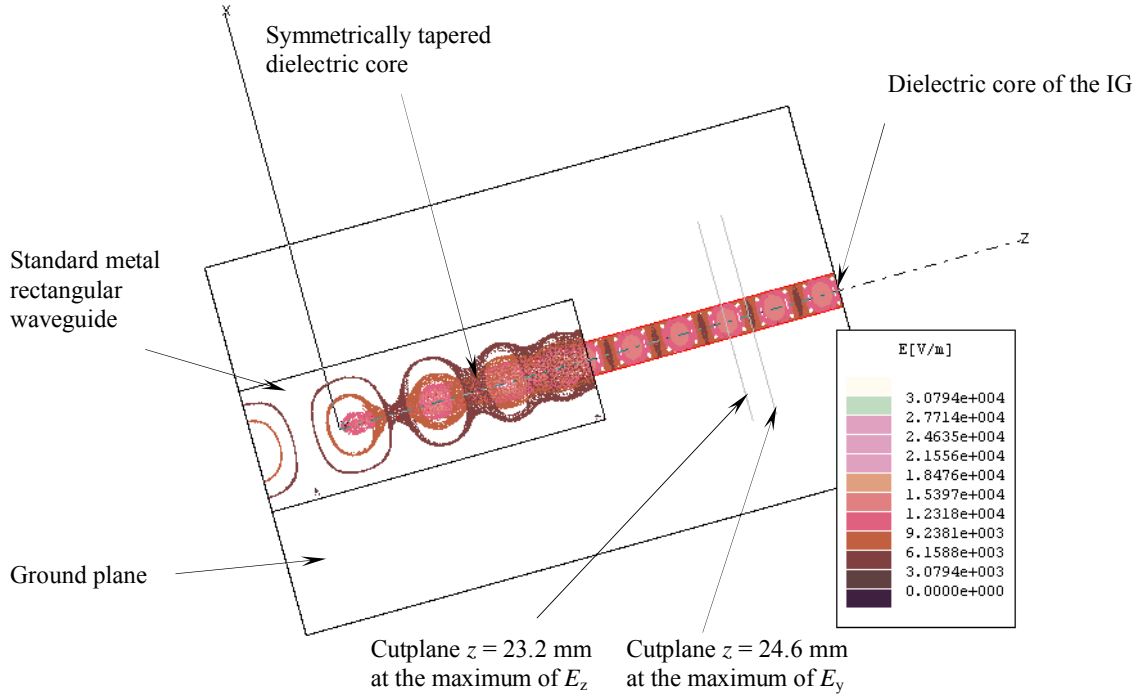


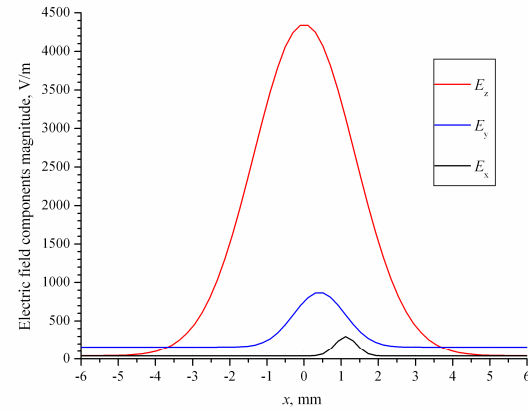
Fig. 5: The simulated distribution of the electric field magnitude in the symmetrical transition with length  $l = 15$  mm.

### III. SIMULATION RESULTS

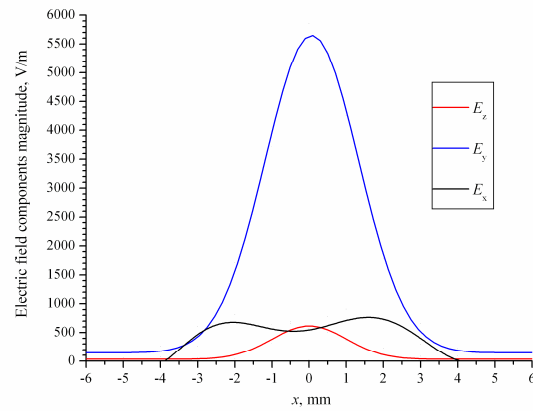
The simulated distribution of the electric field magnitude in the symmetrical transition with length  $l = 15$  mm is shown in the Fig. 5. It is evident the gradual transformation of the dominant mode  $H_{10}$  in the SMRW to the dominant mode in the IG. The field outside the dielectric core of the IG is not shown in Fig. 5 in order to visualize better the distribution inside.

The simulated results for the electric field components at the two cutplanes (Fig. 5),  $z = 23.2$  mm and  $z = 24.6$  mm, are shown in Fig. 6. The former cutplane corresponds to the maximum of both the  $E_z$  component and the magnitude of the electric field, and the latter – to the maximum of the  $E_y$  component. It is evident the asymmetry in the distributions for the  $E_x$  and  $E_y$  components in Fig. 6a, and also in the distribution for the  $E_x$  component in Fig. 6b. This lack of symmetry of the simulated distributions is in agreement with the aforementioned asymmetry in the measured distributions in Fig. 4.

In an attempt to optimize the transition geometry with the help of a 3D electromagnetic simulator [6], [7], we have used the Ansoft HFSS for both the symmetrical and asymmetrical transitions with several taper lengths –  $l = 0, 5, 10, 15, 20$  and  $25$  mm. The results for the scattering parameters  $S_{11}$  and  $S_{21}$  at a frequency of 33 GHz are shown in Table 1. It could be seen, that the symmetrical transitions don't possess better  $S_{11}$  than the asymmetrical ones at every frequency. As a rule, the symmetrical transitions have better  $S_{11}$  at shorter taper lengths, and the asymmetrical transitions – at greater taper lengths. The parameter  $S_{21}$  was better for the symmetrical transitions



(a)



(b)

Fig. 6: The simulated results for the electric field components at (a)  $z = 23.2$  mm (b)  $z = 24.6$  mm.

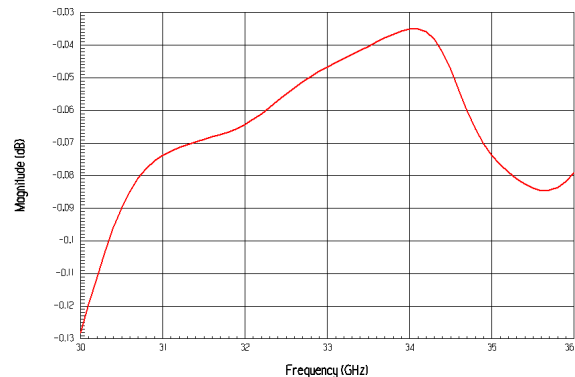
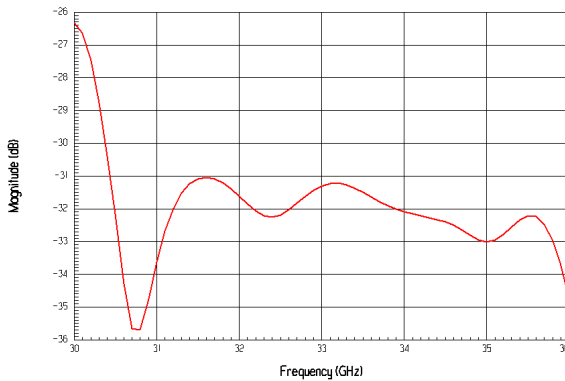


Fig. 7: The simulated results for the scattering parameters  $S_{11}$  (a) and  $S_{21}$  (b) in the frequency range (30 – 36) GHz.

compared to the asymmetrical ones at every taper length.

The frequency dependence of the parameters  $S_{11}$  and  $S_{21}$  in the frequency range (33 – 36) GHz for the symmetrical transition with length  $l = 15$  mm are presented in Fig. 7. The parameter  $S_{11}$  varies between (–0.13 dB) to (–0.035 dB), and the parameter  $S_{21}$  – between (–36 dB) to (–26 dB), which is a rather good performance.

TABLE 1: SIMULATION RESULTS FOR SCATTERING PARAMETEWRS AT DIFFERENT TRANSITION LENGTHS.

Transition configuration	$l$ , mm	$S_{11}$ , dB	$S_{21}$ , dB
Symmetrical	0	- 10.00	- 1.34
	5	- 32.69	- 0.25
	10	- 32.55	- 0.08
	15	- 31.34	- 0.05
	20	- 35.54	- 0.03
Asymmetrical	25	- 35.00	- 0.03
	5	- 30.04	- 0.38
	10	- 33.65	- 0.11
	15	- 32.23	- 0.06
	20	- 35.80	- 0.04
	25	- 37.08	- 0.04

#### IV. CONCLUSION

It could be concluded, that the transitions with lengths equal to two-three guide wavelengths are quite a reasonable choice. The symmetrical tapers perform better than the asymmetrical ones at middle taper lengths.

#### ACKNOWLEDGMENT

The authors thank the Ray Sat Bg Ltd. for the possibility to use the software product Ansoft HFSS.

#### REFERENCES

- [1] S. J. Fiedziuszko, I. C. Hunter, T. Itoh, Y. Kobayashi, T. Nishikawa, S. N. Stitzer and K. Wakino, "Dielectric materials, devices and circuits", *IEEE Trans. Microwave Theory Tech.*, vol. 50, pp. 706 – 720, March 2002.
- [2] Wolfgang Menzel. 2008 August. 50 years of millimeter-waves: A journey of development. *Microwave Journal*. Vol. 51. Available: <http://www.mwjournal.com>
- [3] A. A. Ahumyan, S. S. Gigoyan, B. A. Murmughev and R. M. Martirosyan, "Ferrite isolators for millimeter wavelengths based on the alumina image guide", *Radiotechnics*, pp. 41 – 43, February 1990.
- [4] I. I. Arestova and S. A. Ivanov, "Nonreciprocal effects in coupled ferrite-dielectric image guide structures", in *XII ICMF (International Conference on Microwave Ferrites) Proceedings*, Gyulechica, Bulgaria, 1994, 188-192.
- [5] Iliyana I. Arestova, Plamen I. Dankov and Valda P. Levcheva, "A study on the coupled image guide structures", in *PIERS (Progress In Electromagnetics Research Symposium) Proceedings*, Moscow, 2009, 1204-1209.
- [6] Sergey Dudorov, "Rectangular dielectric waveguide and its optimal transition to a metal waveguide", Ph.D dissertation, Helsinki University of Technology, Helsinki, 2002.
- [7] *Ansoft HFSS User's Manual*, A Full-Wave Spice Problem, 2001.